tvst

Article

Relative Postpartum Retinal Vasoconstriction Detected With Optical Coherence Tomography Angiography

Benjamin R. Lin[1,2], Fei Lin[2], Li Su[3], Marco Nassisi[3], SriniVas R. Sadda[3], Stephanie L. Gaw[4], and Irena Tsui[3]

[1] Bascom Palmer Eye Institute, Miami, FL, USA
[2] David Geffen School of Medicine, Los Angeles, CA, USA
[3] Doheny Eye Center and UCLA Stein Eye Institute, University of California Los Angeles, Los Angeles, CA, USA
[4] Department of Obstetrics, Gynecology & Reproductive Sciences, University of California San Francisco, San Francisco, CA, USA

Correspondence: Irena Tsui, Doris Stein Eye Research Center, University of California Los Angeles, 200 Stein Plaza, Los Angeles, CA 90095-7003, USA. e-mail: itsui@jsei.ucla.edu

Received: October 18, 2020
Accepted: January 18, 2021
Published: February 26, 2021

Keywords: optical coherence tomography angiography; perfusion density; retinal perfusion; vessel length density

Citation: Lin BR, Lin F, Su L, Nassisi M, Sadda SR, Gaw SL, Tsui I. Relative postpartum retinal vasoconstriction detected with optical coherence tomography angiography. Trans Vis Sci Tech. 2021;10(2):40, https://doi.org/10.1167/tvst.10.2.40

Purpose: To characterize changes in retinal perfusion during pregnancy and the postpartum period using optical coherence tomography angiography (OCTA).

Methods: A nonmydriatic OCTA camera was used to image healthy women who were pregnant or in the postpartum period along with nonpregnant controls. Perfusion density (PD) and vessel length density (VLD) in the superficial capillary plexus (SCP), intermediate capillary plexus (ICP), and deep capillary plexus (DCP) were evaluated.

Results: A total of 16, 15, and 13 eyes from nonpregnant, pregnant, and healthy postpartum subjects, respectively, were evaluated. When compared to controls, there were significant increases in ICP PD during the second and third trimester of pregnancy, along with significant decreases in both PD and VLD in SCP, ICP, and DCP up to 14 weeks postpartum.

Conclusions: During pregnancy, vascular changes consistent with retinal vasodilation were noted in the ICP. During the postpartum period, changes in retinal vasculature suggest relative vasoconstriction involving all three layers when compared to both the pregnant and nonpregnant states.

Translational Relevance: Detecting postpartum changes in retinal vasculature could offer important insights into postpartum physiology throughout the body.

Introduction

Hemodynamic changes occur in every organ system during pregnancy to support placental circulation and fetal development. By the third trimester of pregnancy, mothers experience overall decreases in blood pressure that are offset by increases in stroke volume and cardiac output to maintain adequate perfusion.[1–4] The physiologic changes in blood pressure are partially due to a decrease in systemic vascular resistance secondary to hormonal effects from estrogen, progesterone, prostaglandins, and prolactin.[5–7] The effects of these four systemically circulating hormones may also have a significant effect on retinal vasculature.

Imaging of the retinal vasculature during pregnancy has been limited due to concerns regarding the use of mydriatic eye drops and fluorescein dye, which are both categorized as pregnancy category C. In addition, phenylephrine given systemically for anesthesia has been associated with decreased uteroplacental perfusion, with potentially increased risk in the setting of acute or chronic placental insufficiency.[8] Although fluorescein angiography does not have documented teratogenic effects, it has not been studied in pregnancy and can cause nausea and vomiting in a small subset of subjects.[9,10]

A better understanding of the normal vascular changes that occur within the eye during pregnancy would be helpful to understand retinal diseases in pregnancy and to evaluate the retina as a potential

Copyright 2021 The Authors

This work is licensed under a Creative Commons Attribution-NonCommercial-NoDerivatives 4.0 International License.

biomarker for abnormal pregnancies. The purpose of this study was to characterize retinal vascular changes in pregnancy by longitudinally assessing data during pregnancy and in the postpartum period.

Materials and Methods

The study sites included the Doheny UCLA Eye Centers (Pasadena, CA) and the Ronald Reagan UCLA Medical Center (Los Angeles, CA). The research followed the tenets of the Declaration of Helsinki. Research was approved by the institutional review board at the University of California, Los Angeles. Informed consent was obtained from subjects after explanation of the nature and possible consequences of the study.

Women with uncomplicated pregnancies in their second trimester were recruited and imaged during the second or third trimester of pregnancy and/or 3 months postpartum. Exclusion criteria included eyes with refractive error greater than –6.00 diopters spherical equivalent, history of ocular disease other than refractive error, and history of hypertension, diabetes, or other systemic illness. An age-matched control group of nonpregnant healthy women was recruited with the same exclusion criteria. All subjects had both eyes imaged.

Imaging was performed without pharmacologic dilation after the patient was allowed to rest in a dark room for at least 5 minutes. Spectral-domain optical coherence tomography angiography (OCTA) imaging of all subjects was performed with Spectralis OCT (Heidelberg Engineering, Heidelberg, Germany). The camera was aligned through the pupil, and images were acquired at 512 A-scans/B-scan by 512 B-scans/volume with scan sizes of 10° by 10°. Automated segmentation was performed using the Heidelberg Spectralis software from the inner limiting membrane to the retinal pigment epithelium. En face angiograms of the autosegmented superficial capillary plexus (SCP), intermediate capillary plexus (ICP), and the deep capillary plexus (DCP) were exported with projection artifacts automatically corrected for by the Heidelberg software. The SCP was autosegmented to include the nerve fiber layer and ganglion cell layer. The ICP was auto-segmented to include the deep portion of the inner plexiform layer and the superficial portion of the inner nuclear layer. The DCP was autosegmented to include the deep portion of the inner nuclear layer and the outer plexiform layer. ImageJ 1.52n (National Institutes of Health, Bethesda, MD) was used to binarize the images and calculate vessel perfusion density (PD) and vessel length density (VLD) in accordance with previously published techniques.[11] PD refers to the total area covered by perfused vasculature, whereas VLD excludes cross-sectional area to measure only the total length of the vasculature. The area of the black pixels of the binarized image is summed to calculate the vessel PD. The image is subsequently skeletonized to one pixel area in width and the area calculated again to determine VLD (Fig. 1). PD and VLD values were computed in seven zones for each layer: (1) whole image (entire field of view); (2) fovea (circle centered on the fovea with 0.5-mm radius); (3) parafovea (ring centered on the fovea with inner and outer radii of 0.5 and 1.5 mm, respectively); and (4–7) superior, inferior, nasal, and temporal inner macula subfields per the Early Treatment Diabetic Retinopathy Study (ETDRS) grid (Fig. 1). Computing PD and VLD values for seven zones in each of the three layers yielded a total of 42 values per image.

Prior to statistical analysis, the data were filtered. Eyes were further excluded if the signal strength was lower than 30 dB or if there was significant motion, imaging artifact, or segmentation error leading to a loss of B-scan imaging data. A subset of subjects also had postpartum imaging performed for comparison. Statistical analysis was performed using Stata (StataCorp, College Station, TX). We compared each parameter at each location in each layer among three groups (i.e., nonpregnant, pregnant, postpartum)—an analysis of variance type of comparison without any other potential confounders in the model. Generalized estimating equations were used to correct for potential correlations between two eyes from the same patient ($P < 0.05$ was considered significant).

Results

A total of 62 eyes were imaged. After exclusion criteria were applied, a total of 44 eyes were included in the analyses: 16 nonpregnant controls, 15 pregnant, and 13 postpartum eyes (Fig. 2). The difference between the number of pregnant and postpartum eyes imaged is due to patients being lost to follow-up or declining imaging at their postpartum visit. The average ages of nonpregnant, pregnant and postpartum eyes were 36.1, 31.6, and 34.4 years, respectively, which were not significantly different ($P > 0.05$ among all groups). The pregnant eyes were imaged at an average of 24.6 weeks (SD, ±8.5) of gestation, and the postpartum eyes were imaged at an average of 10.6 weeks (SD, ±3.63) after delivery. Average scan quality (dB) values for the nonpregnant control, pregnant, and postpartum

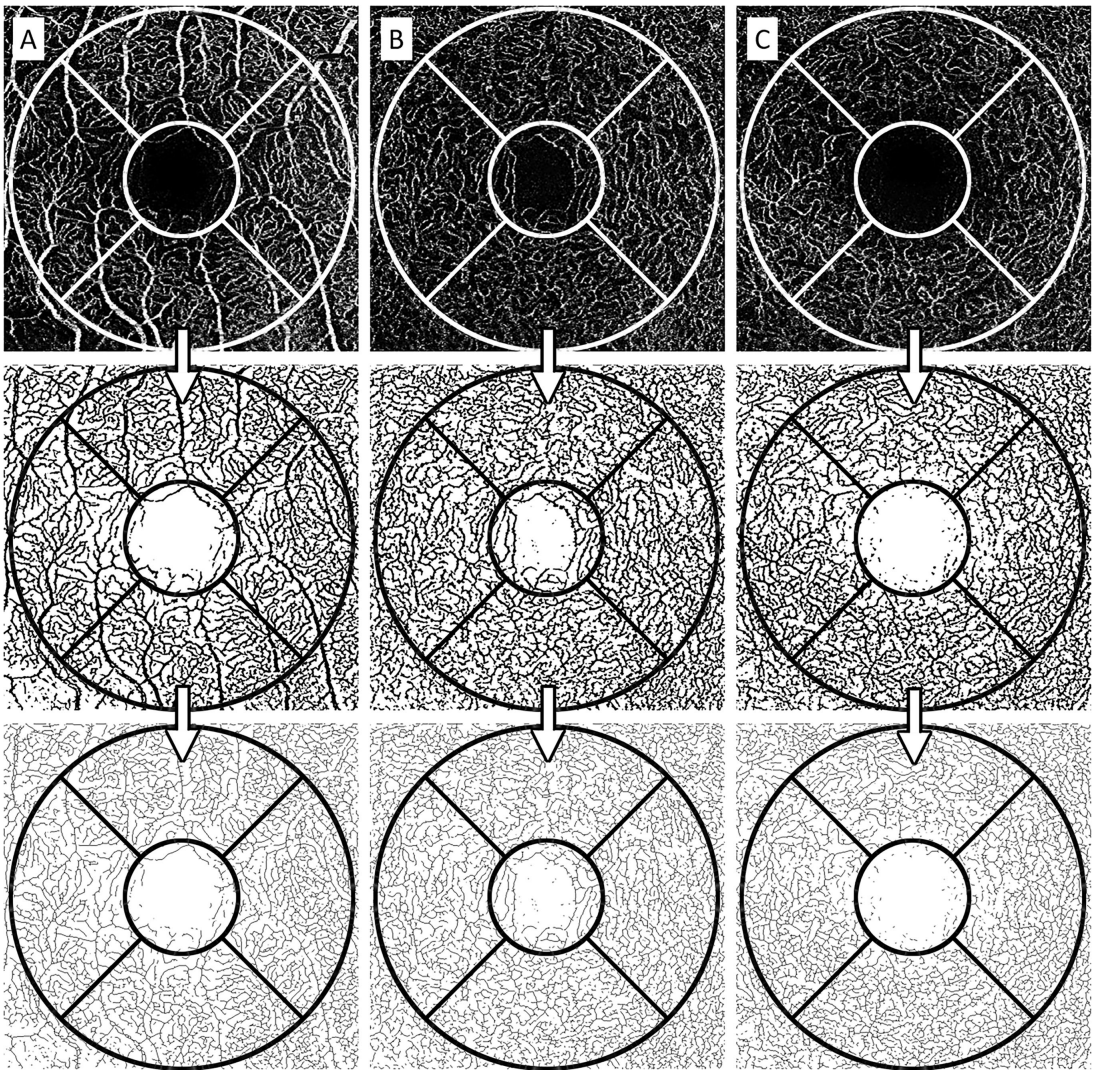

Figure 1. Processing of representative images. Images are shown from the SCP (*column A*), ICP (*column B*), and DCP (*column C*). ETDRS subfields (*white* and *black rings*) are overlaid on the image and centered over the fovea (*row 1*). The area of the *black pixels* of the binarized image (*row 2*) is summed to calculate the vessel PD. The image was subsequently skeletonized and the area calculated again to determine vessel length density (*row 3*).

eyes were 34.6 ± 3.2, 36.4 ± 3.0, and 35.4 ± 3.0, respectively ($P = 0.16$). Average spherical equivalents of nonpregnant control, pregnant, and postpartum eyes were –0.45 ± 1.0, –2.06 ± 2.1, and –1.85 ± 2.1. Only the nonpregnant control and pregnant groups showed a statistically significant difference ($P < 0.05$) in spherical equivalent. There was no difference in refractive error between the pregnant and postpartum groups or the nonpregnant and postpartum groups ($P > 0.05$). Blood pressure was normal at all study visits. All eyes had best-corrected visual acuity of 20/20.

Comparison of Nonpregnant, Pregnant, and Postpartum Eyes

Generalized estimating equation analysis of all three groups of subjects showed significant differences in multiple regions in both PD and VLD across all capillary beds: SCP, ICP, and DCP. This included three regions in SCP, eight regions in ICP, and six regions in DCP (Table 1). In general, all three layers were either significant for or trended toward increases during pregnancy and decreases during the postpartum period when compared to nonpregnant controls.

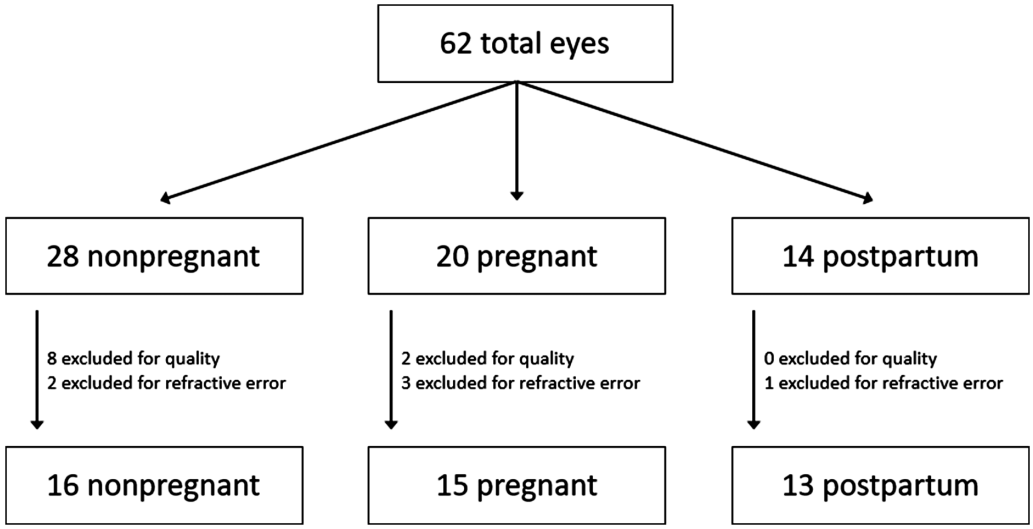

Figure 2. Flowchart showing number of eyes included and excluded. A total of 62 eyes were imaged, and 44 were included in the final analysis.

Superficial Capillary Plexus

None of the SCP PD or SCP VLD fields showed significant changes when comparing pregnant with nonpregnant groups (Table 1). However, most of the values trended toward an increase in pregnancy. In addition, one of the seven SCP PD and six of the seven SCP VLD fields showed a significant decrease in the postpartum group when compared to the pregnancy group. Finally, four of the seven SCP PD fields showed a significant decrease in the postpartum period when compared to the nonpregnant controls. A subset of subjects was imaged twice at both the intrapartum and postpartum time periods (Table 2). Statistics were not run on these patients due to the small sample size, but the vast majority of all PD and VLD values trended in the same direction, with decreases in the postpartum period.

Intermediate Capillary Plexus

Four of the seven ICP PD fields and one of the seven ICP VLD fields showed a significant increase in the pregnant group when compared to the nonpregnant group (Table 1). In addition, three of the seven ICP PD fields and four of the seven ICP VLD fields showed a significant decrease in the postpartum group when compared to the pregnant group. Finally, three of the seven ICP VLD fields showed a significant decrease in the postpartum group when compared to the nonpregnant group.

Deep Capillary Plexus

Similarly to the SCP, none of the fields in DCP PD or DCP VLD showed significant changes in the pregnant group when compared to the nonpregnant group (Table 1). However, all of the fields in the postpartum group showed significant changes when compared to both nonpregnant and pregnant groups. When compared to the nonpregnant group, four of the seven DCP PD fields and six of the seven DCP VLD fields showed a significant decrease in the postpartum group. Additionally, all seven of the DCP PD fields and six of the seven DCP VLD fields showed a significant decrease when compared to the nonpregnant group.

Discussion

In addition to evaluating postpartum retinal vasculature for the first time, to our knowledge, this study corroborates work done previously by our group using the RTVue XR Avanti OCTA (Optovue, Fremont, CA) during pregnancy itself.[11] The prior study found increases in the DCP during pregnancy; however, the DCP included the ICP, as autosegmentation performed by the Avanti OCT software did not allow discrimination between the two plexuses. The present study further localizes the apparent intrapartum retinal vascular changes, showing an increase at the level of the ICP, but not the DCP, during pregnancy.

Ex-vivo confocal microscopy of the macula has demonstrated that arterioles are more superficial than

Table 1. Comparing Nonpregnant, Pregnant, and Postpartum Eyes

Layer and ETDRS Subfield	Perfusion Density (Mean ± SD)				Vessel Length Density (Mean ± SD)			
	Nonpregnant (n = 16)	Pregnant (n = 15)	Postpartum (n = 13)	*P*	Nonpregnant (n = 16)	Pregnant (n = 15)	Postpartum (n = 13)	*P*
SCP								
Total	32.59 ± 1.22	33.26 ± 1.48	31.95 ± 1.85	0.209	8.34 ± 0.43	8.36 ± 0.84	7.80 ± 0.57†	0.067
1 mm	9.54 ± 4.00	13.51 ± 5.16	10.11 ± 5.76	0.168	2.28 ± 0.95	3.24 ± 1.32	2.42 ± 1.40	0.193
Parafoveal	35.04 ± 1.22	35.42 ± 1.40	33.70 ± 1.60*,†	0.031‡	8.81 ± 0.45	8.76 ± 0.93	8.11 ± 0.60†	0.015‡
Superior	35.56 ± 1.51	35.83 ± 1.42	34.27 ± 2.22*	0.073	8.94 ± 0.48	8.88 ± 0.83	8.31 ± 0.76†	0.077
Nasal	35.23 ± 2.01	35.47 ± 1.59	33.87 ± 2.24*	0.055	8.85 ± 0.67	8.79 ± 0.90	8.22 ± 0.74†	0.046†
Temporal	34.54 ± 2.21	35.24 ± 1.80	32.83 ± 1.63*	0.010‡	8.53 ± 0.67	8.57 ± 1.08	7.77 ± 0.59†	0.014‡
Inferior	34.82 ± 1.64	35.24 ± 1.80	33.83 ± 1.86	0.202	8.92 ± 0.52	8.80 ± 1.06	8.15 ± 0.68†	0.020‡
ICP								
Total	31.63 ± 1.42	33.29 ± 1.41†	31.76 ± 1.75*	0.005‡	8.45 ± 0.47	8.59 ± 0.47	8.05 ± 0.48*	0.041‡
1 mm	16.98 ± 4.12	23.42 ± 4.01†	18.57 ± 6.01	0.002‡	4.16 ± 1.10	5.62 ± 1.13†	4.34 ± 1.50	0.011†
Parafoveal	33.16 ± 1.55	34.25 ± 1.07†	32.82 ± 1.36*	0.007‡	8.68 ± 0.50	8.67 ± 0.47	8.17 ± 0.50*,†	0.038‡
Superior	33.31 ± 2.31	33.70 ± 1.84	32.60 ± 2.19	0.300	8.78 ± 0.67	8.64 ± 0.50	8.21 ± 0.74	0.152
Nasal	33.60 ± 3.15	34.88 ± 2.03	33.95 ± 1.64	0.266	8.68 ± 0.96	8.75 ± 0.66	8.39 ± 0.62	0.269
Temporal	33.48 ± 2.47	34.86 ± 1.25†	32.95 ± 1.35*	0.001‡	8.67 ± 0.70	8.71 ± 0.50	8.06 ± 0.39*,†	0.002‡
Inferior	32.18 ± 2.41	33.39 ± 1.61	31.76 ± 2.33	0.053	8.59 ± 0.65	8.60 ± 0.60	8.01 ± 0.69*,†	0.084
DCP								
Total	32.16 ± 2.23	33.08 ± 1.62	30.74 ± 1.88*	0.003‡	8.62 ± 0.67	8.69 ± 0.58	7.89 ± 0.52*,†	0.001‡
1 mm	7.75 ± 4.84	11.76 ± 5.29	6.62 ± 4.24*	0.081	1.99 ± 1.16	3.00 ± 1.37	1.73 ± 1.10*	0.097
Parafoveal	34.50 ± 2.40	34.83 ± 1.22	32.26 ± 1.66*,†	<0.001†	9.03 ± 0.71	8.97 ± 0.60	8.15 ± 0.72*,†	0.006‡
Superior	34.49 ± 2.72	34.22 ± 2.05	31.76 ± 2.08*,†	0.001‡	9.12 ± 0.87	8.91 ± 0.72	8.17 ± 0.83*,†	0.016‡
Nasal	35.51 ± 2.77	35.49 ± 1.90	33.56 ± 3.35*,†	0.023‡	9.17 ± 0.74	9.08 ± 0.68	8.42 ± 1.14†	0.076
Temporal	34.35 ± 3.64	35.09 ± 1.77	31.60 ± 1.98*,†	<0.001‡	8.89 ± 1.00	8.92 ± 0.73	7.86 ± 0.75*,†	0.004‡
Inferior	33.59 ± 2.65	34.28 ± 1.77	32.10 ± 2.72*	0.017‡	8.95 ± 0.81	8.96 ± 0.71	8.17 ± 0.84*,†	0.014‡

P values indicate statistical significance across all three groups as calculated by generalized estimating equations.
*$P < 0.05$ compared with pregnant group.
†$P < 0.05$ compared with nonpregnant group.
‡$P < 0.05$ compared across all three groups.

Table 2. Longitudinal Data for Four Women Who Were Imaged During Pregnancy and Postpartum

Layer and ETDRS Subfield	Perfusion Density (Mean ± SD)		Vessel Length Density (Mean ± SD)	
	Pregnant	Postpartum	Pregnant	Postpartum
SCP				
Total	33.47 ± 0.86	32.75 ± 0.69	8.37 ± 0.56	7.82 ± 0.31
1 mm	13.54 ± 4.41	10.70 ± 4.17	3.18 ± 1.12	2.52 ± 1.01
Parafoveal	35.46 ± 1.32	34.10 ± 0.98	8.70 ± 0.73	8.04 ± 0.39
Superior	34.32 ± 1.74	34.85 ± 0.95	8.57 ± 0.61	8.19 ± 0.52
Nasal	35.84 ± 1.83	34.27 ± 1.79	8.84 ± 0.77	8.15 ± 0.48
Temporal	35.49 ± 1.74	33.12 ± 1.17	8.54 ± 0.82	7.69 ± 0.50
Inferior	36.20 ± 2.09	34.20 ± 1.51	8.85 ± 0.90	8.15 ± 0.51
ICP				
Total	33.15 ± 0.72	32.63 ± 0.88	8.58 ± 0.34	7.97 ± 0.32
1 mm	21.11 ± 4.39	19.08 ± 4.39	4.96 ± 1.17	4.40 ± 1.06
Parafoveal	34.30 ± 0.67	33.27 ± 1.09	8.69 ± 0.33	8.00 ± 0.35
Superior	32.70 ± 2.26	33.26 ± 1.26	8.43 ± 0.45	8.05 ± 0.48
Nasal	35.44 ± 1.14	34.18 ± 1.37	8.93 ± 0.52	8.20 ± 0.48
Temporal	35.44 ± 0.83	33.25 ± 1.42	8.77 ± 0.32	7.86 ± 0.26
Inferior	33.61 ± 0.96	32.41 ± 1.74	8.64 ± 0.41	7.89 ± 0.49
DCP				
Total	33.02 ± 0.74	31.41 ± 1.50	8.65 ± 0.52	7.72 ± 0.36
1 mm	9.98 ± 5.29	7.23 ± 3.92	2.50 ± 1.37	1.83 ± 0.98
Parafoveal	34.71 ± 1.29	32.09 ± 1.50	8.90 ± 0.64	7.78 ± 0.46
Superior	34.57 ± 1.43	32.04 ± 1.55	8.99 ± 0.23	7.85 ± 0.51
Nasal	36.54 ± 2.04	32.91 ± 3.01	9.27 ± 0.85	7.92 ± 0.78
Temporal	34.27 ± 2.13	31.54 ± 2.29	8.61 ± 0.76	7.57 ± 0.75
Inferior	33.48 ± 2.42	31.90 ± 2.37	8.74 ± 0.91	7.79 ± 0.53

The perfusion density and vessel length density data for the seven eyes from four women who were imaged at both the intrapartum and postpartum time periods show similar trends as found in Table 1. *P* values were not calculated due to the small sample size.

venules.[12] In addition, the superficial, intermediate, and deep vascular plexuses are a complex network of vessels that are primarily connected in series, rather than in parallel, from superficial to deep, with arterial inflow occurring mainly at the SCP and venous outflow occurring primarily at the DCP.[12] We speculate that localization to the ICP may have to do with the nature of the vertical anastomoses that the ICP has with the SCP and DCP or the composition or diameter of vessels within each layer and the subsequent effects on vascular resistance. However, more studies must be performed to better understand these changes.

Previous studies with nonmydriatic retinal cameras have shown retinal vascular changes in pregnancy reported as central retinal arteriolar equivalents (CRAEs) and central retinal venular equivalents (CRVEs), calculated values that act as a surrogate for the central retinal artery and vein calibers. Lupton et al.[13] found increases in CRAE and CRVE in the early second trimester that returned to baseline in the late second trimester through delivery. These changes corresponded to a decrease in systemic mean arterial pressure (MAP) in the second trimester. The subclinical retinal vasodilation we noted in our pregnancy group compared with the non-pregnant group was consistent with the previously reported increases in CRAE and CRVE.

To our knowledge, this is the first study that has compared postpartum retinal vasculature to that of the normal pregnant and nonpregnant states using OCTA. In our study during the postpartum period, most fields demonstrated significant decreases in both PD and VLD values when compared to both the pregnant and nonpregnant states. PD is calculated after binarizing the en face image and summing the area covered by

blood vessels. VLD is calculated in a similar fashion but also involves skeletonizing retinal vessels to 1 pixel width.

There are three reasons why decreases in both PD and VLD may be seen in a relatively short time period. First, it is possible that the decreases in postpartum VLD values that we observed were due to vasoconstriction of the most distal retinal blood vessels below the detection threshold, which would lead to capillary dropout on imaging and apparent loss of vessel length. Second, true blood vessel regression could also be occurring secondary to elevated antiangiogenic vasoinhibins that are derived from elevated levels of retinal prolactin in the postpartum state. Third, a decrease in VLD may be related to a change in blood vessel morphology. An increase in vessel tortuosity would lead to an increase in apparent VLD. In a large association study, an increase in blood vessel tortuosity was found to correlate with increases in systolic blood pressure and MAP.[14] Although all subjects were normotensive, we hypothesize that our findings are due to a relative decrease in blood pressure and MAP postpartum, leading to decreased VLD in the retina.

Systemically, postpartum vasoconstriction increases total peripheral vascular resistance to reduce the risk of hypotension secondary to intrapartum blood loss.[15–17] These changes may continue for several months after delivery.[16] This is consistent with our findings of relative retinal vasoconstriction 14 weeks postpartum. Future research is needed to determine if and when this retinal vasoconstriction returns to baseline levels seen in nonpregnant states.

A limitation of this study is the small number of subjects with postpartum follow-up and the single postpartum time point. Future studies with multiple and longer postpartum follow-up would better establish a clear longitudinal trend in vascular changes. Nonetheless, even with a small number of subjects, we showed a consistent difference in retinal perfusion in subjects who were imaged in the postpartum time period. A second limitation of this study is that the pregnant subjects were slightly more myopic than the nonpregnant controls; however, this would result in lower retinal measurements in pregnancy and underestimate the differences found in the study.[18]

In conclusion, this study demonstrated relative retinal vasoconstriction in postpartum women in all three OCTA-discernable capillary layers. Comparing data from pregnant to nonpregnant control groups suggests a relative retinal vasodilation during pregnancy primarily affecting the ICP, but not the SCP or DCP. Future studies can consider imaging subjects at multiple intrapartum and postpartum time points.

Acknowledgments

Supported by a grant from the National Institutes of Health (R21EY03029501A1) and by Research to Prevent Blindness. The funding organizations had no role in the design or conduct of this research, including study design, data collection, data analysis, or manuscript preparation.

Disclosure: **B.R. Lin,** None; **F. Lin,** None; **L. Su,** None; **M. Nassisi,** None; **S.R. Sadda,** Heidelberg Engineering (F), Optos (F), CenterVue (F), Nidek (F, S), Topcon (F, S), Carl Zeiss Meditec (R, S); **S.L. Gaw,** None; **I. Tsui,** None

References

1. Ouzounian JG, Elkayam U. Physiologic changes during normal pregnancy and delivery. *Cardiol Clin.* 2012;30(3):317–329.
2. McLaughlin K, Audette MC, Parker JD, Kingdom JC. Mechanisms and clinical significance of endothelial dysfunction in high-risk pregnancies. *Can J Cardiol.* 2018;34(4):371–380.
3. Kovo M, Schreiber L, Bar J. Placental vascular pathology as a mechanism of disease in pregnancy complications. *Thromb Res.* 2013;131(suppl 1):S18–S21.
4. Roberts JM. Pathophysiology of ischemic placental disease. *Semin Perinatol.* 2014;38(3):139–145.
5. Greiss FC, Jr, Anderson SG. Effect of ovarian hormones on the uterine vascular bed. *Am J Obstet Gynecol.* 1970;107(6):829–836.
6. Gerber JG, Payne NA, Murphy RC, Nies AS. Prostacyclin produced by the pregnant uterus in the dog may act as a circulating vasodepressor substance. *J Clin Invest.* 1981;67(3):632–636.
7. Bryant EE, Douglas BH, Ashburn AD. Circulatory changes following prolactin administration. *Am J Obstet Gynecol.* 1973;115(1):53–57.
8. Ngan Kee WD, Khaw KS, Tan PE, Ng FF, Karmakar MK. Placental transfer and fetal metabolic effects of phenylephrine and ephedrine during spinal anesthesia for cesarean delivery. *Anesthesiology.* 2009;111(3):506–512.
9. Halperin LS, Olk RJ, Soubrane G, Coscas G. Safety of fluorescein angiography during pregnancy. *Am J Ophthalmol.* 1990;109(5):563–566.

10. Kwan AS, Barry C, McAllister IL, Constable I. Fluorescein angiography and adverse drug reactions revisited: the Lions Eye experience. *Clin Exp Ophthalmol.* 2006;34(1):33–38.
11. Chanwimol K, Balasubramanian S, Nassisi M, et al. Retinal vascular changes during pregnancy detected with optical coherence tomography angiography. *Invest Ophthalmol Vis Sci.* 2019;60(7):2726–2732.
12. An D, Yu P, Freund KB, Yu DY, Balaratnasingam C. Three-dimensional characterization of the normal human parafoveal microvasculature using structural criteria and high-resolution confocal microscopy. *Invest Ophthalmol Vis Sci.* 2020;61(10):3.
13. Lupton SJ, Chiu CL, Hodgson LA, et al. Temporal changes in retinal microvascular caliber and blood pressure during pregnancy. *Hypertension.* 2013;61(4):880–885.
14. Tapp RJ, Owen CG, Barman SA, et al. Associations of retinal microvascular diameters and tortuosity with blood pressure and arterial stiffness: United Kingdom Biobank. *Hypertension.* 2019;74(6):1383–1390.
15. Morris R, Sunesara I, Rush L, et al. Maternal hemodynamics by thoracic impedance cardiography for normal pregnancy and the postpartum period. *Obstet Gynecol.* 2014;123(2 pt 1):318–324.
16. San-Frutos L, Engels V, Zapardiel I, et al. Hemodynamic changes during pregnancy and postpartum: a prospective study using thoracic electrical bioimpedance. *J Matern Fetal Neonatal Med.* 2011;24(11):1333–1340.
17. Lavie A, Ram M, Lev S, et al. Maternal hemodynamics in late gestation and immediate postpartum in singletons vs. twin pregnancies. *Arch Gynecol Obstet.* 2018;297(2):353–363.
18. Su L, Ji YS, Tong N, et al. Quantitative assessment of the retinal microvasculature and choriocapillaris in myopic patients using swept-source optical coherence tomography angiography. *Graefes Arch Clin Exp Ophthalmol.* 2020;258(6):1173–1180.